NUCL SCI TECH (2017) 28:60
DOI 10.1007/s41365-017-0210-2

# Scan system for arbitrary-shaped samples at the synchrotron radiation facility

**Xu-Ying Lan[1] · Dong-Xu Liang[1] · Cheng-Wen Mao[1]**

Received: 7 September 2016 / Revised: 31 October 2016 / Accepted: 2 November 2016 / Published online: 28 March 2017


**Abstract** X-ray fluorescence (XRF) scan methodology is important for elemental mapping of samples at a synchrotron radiation facility. To save the experiment time and improve the experiment efficiency, one should develop an efficient XRF scan method. In this paper, a new scan mode is presented. It can map arbitrary-shaped areas without stopping the motors. The control and data acquisition system integrates motor controlling, detector triggering, and data acquisition and storage. The system realizes the arbitrary-shaped 2D-mapping and fluorescence data acquisition synchronously. SR-XRF mapping has been performed with a standard gold mask to verify the validity of this method at beamline BL15U1 of the Shanghai Synchrotron Radiation Facility. The results show that this method reduces the total scan time and improves the experiment efficiency.

**Keywords** Synchrotron radiation · X-ray fluorescence mapping · EPICS · XPS controller

## 1 Introduction

Synchrotron radiation X-ray fluorescence (SR-XRF), a non-destructive technique for elemental mapping of a sample, is widely used in biology, materials science and environmental science [1–4]. It is important for a synchrotron radiation facility to develop XRF scan methodology, a key factor for elemental imaging and the success of experiments. However, conventional XRF scan methods often waste precious beam time due to scanning areas in a simple grid that is large enough to include an irregular-shaped sample or turning on and off the stepper motors. To meet the users' rising demands for beam time of a synchrotron radiation facility, it is critical to improve XRF methodology and the experiment efficiency [5–9].

Researching XRF scan methodology based on Experimental Physics and Industrial Control System (EPICS) software platform has been developed in the synchrotron radiation community. To increase mapping efficiency, 'on-the-fly' scan mode, in which motors continuously move without stopping, has been developed [10–13]. However, this rectangle scan mode still wastes much time on mapping uninterested areas of a sample. Although a 'table mode' scan can achieve arbitrary-shaped area mapping, it has to stop at the end of each motion and this takes time. So it is imperative to develop a mapping method to scan an irregular-shaped sample, rather than mapping a rectangle area, without stopping the motors.

In this paper, for realizing continuously mapping arbitrary-shaped samples, a scan system is implemented at beamline BL15U1 of the Shanghai Synchrotron Radiation Facility (SSRF). The architecture and design of this scan system are provided. Trajectory definition and motion control are built to control sample stage motors moving along the set of mapping trajectory. Scan programs are compiled for the pixel positions and fluorescence data acquisition synchronously. As an example, the elemental distributions of an irregular-shaped area in a standard gold mask are determined. The validity of this technique is confirmed by comparing the original sample image obtained by an optical microscope. By comparing with the

✉ Xu-Ying Lan
lanxuying@sinap.ac.cn

1 Shanghai Institute of Applied Physics, Chinese Academy of Sciences, Zhangjiang Campus, Shanghai 201204, China

XRF scan methods of 'step-by-step,' 'on-the-fly' and 'table modes,' the present method is more efficient.

## 2 Methods

### 2.1 Method architecture

XRF analysis determines the elemental distributions of a sample by measuring the fluorescent (or secondary) X-ray emitted from a sample excited by a primary X-ray source [14, 15]. According to the XRF principle, an XRF scan system for arbitrary-shaped samples is developed on the basis of the scanning XRF microprobe. It mainly consists of mapping area selection, trajectory motion control and fluorescence data acquisition. The scanning XRF microprobe at BL15U1 is shown schematically in Fig. 1. An optical microscope with a charge-coupled device (CCD) camera is used to observe the sample and select the fluorescent mapping areas. The sample stage motors perform high-precision motions in $X$–$Y$ directions in constant speed. The XPS controller connected to a SLS2015 stepper motor driver is capable of executing complex coordinated motions. The Si drifting detector (SDD) collects energy-dispersive XRF counts, and the data are processed by a Saturn device. Two ionization chambers positioned upstream and downstream of the sample monitor intensities of the incident and transmitted X-ray beam.

After selecting scan area of an arbitrary-shaped sample through the microscope CCD camera, a scan trajectory-defined file, which can be read by the XPS controller, is created. After uploading the trajectory file to the controller and setting scan parameters, the XPS controller controls the $X$–$Y$ stage motors to move along the defined trajectory within the sample. The sample is continuously scanned, while the $X$–$Y$ motor position values and corresponding XRF spectrum of each pixel are recorded. Based on the scan data, a two-dimensional fluorescent image of the arbitrary-shaped sample can be obtained.

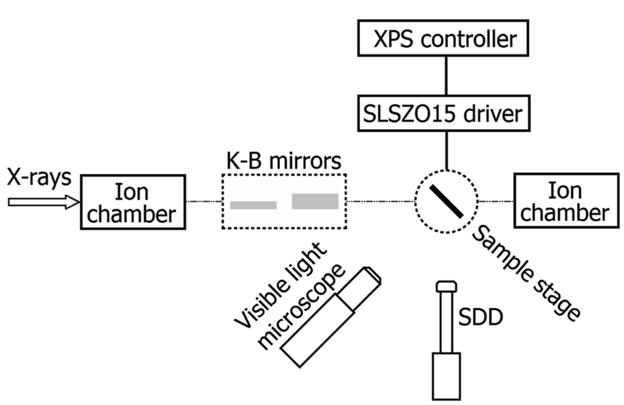


**Fig. 1** Plan view of XRF microprobe for scanning arbitrary-shaped samples

### 2.2 Trajectory definition and motion control

In this XRF mapping system, for scanning an irregular shape, some trajectories are defined to move the stage motors through a set of complex motions. In order to realize motors moving continuously from beginning to the end without stopping, the line–arc trajectory function of XPS is used to do motion control in which an element of a trajectory is defined by a line or an arc segment as shown in Fig. 2 [16]. A line element is defined by specifying the ending point ($X_i$, $Y_i$). The element starting point is the end point of the previous segment ($X_{i-1}$, $Y_{i-1}$). All line element positions are defined relative to the trajectory starting point (0, 0). An arc is defined by specifying radius $R$ and sweep angle $A$ like $Arc(R, A)$. Positive angles are measured counterclockwise.

For hardware configuration, the XPS-DRV00 is a pass-through board used for external amplifiers connected to the XPS controller. This pass-through module passes control signals to the external third-party SLS2015 drivers. Based on the motor driver model and the trajectory definition file, the XPS controls the sample stage motors moving along the specified path.

### 2.3 Scan program

All the data acquisition and control system run on the EPICS software platform at BL15U1 [17, 18]. In this scan system, a scan program is compiled with EPICS to achieve 2D-mapping of a given shape and XRF data acquisition synchronously. For obtaining pixel positions and corresponding XRF data synchronously, a distributed soft real-time control system is built.

For XRF data acquisition, scan programs employ SSCAN and SEQ packages to trigger SDD, record detector data and motor positions of each pixel. The trigger of detector in a scan refers to a process variable (PV) to do data acquisition including XRF spectrum, flux and motor positions by writing to the detector trigger fields in the

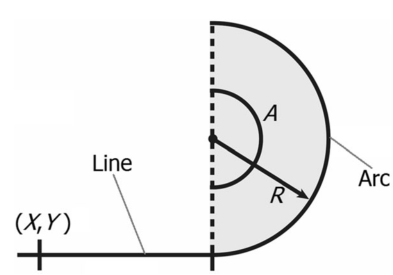


**Fig. 2** Line–arc trajectory definition

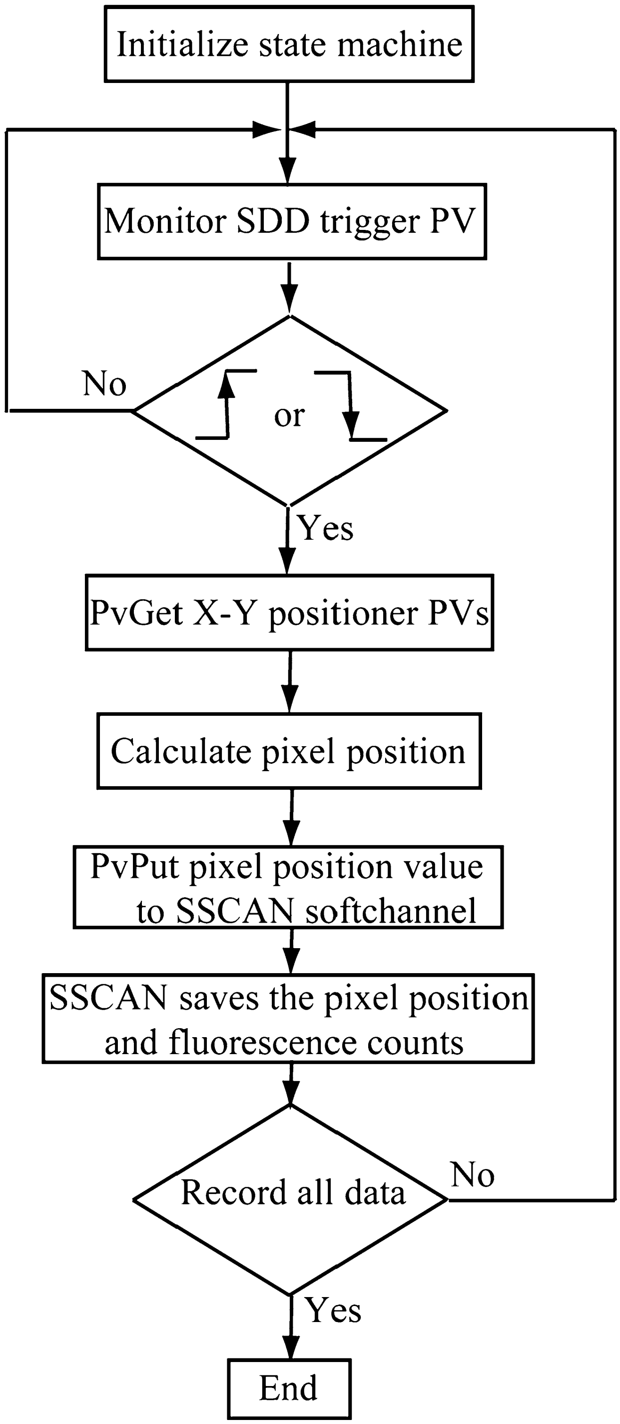


**Fig. 3** Flow chart of the data acquisition

SSCAN. The XRF data acquisition is realized by writing SDD multichannel analysis (MCA) PV into the field of SSCAN. For recording a set of *X*–*Y* motor positions, some soft channels are built in the SSCAN db file, which saves the *X* and *Y* motor positions of each pixel. Their values are real-time obtained by using SEQ.

Underlying the SSCAN software, SEQ and state notation language (SNL) are applied to create distributed soft real-time control systems for scaling scientific instruments [19, 20]. It is easy for the program to interact with EPICS PVs, and it allows to read and write PVs and to react to changes in their values or status. A state machine is defined to get the pixel positions depending on the SDD trigger signals. Whenever the values of motor positions and SDD trigger signals in the control system (the EPICS database) change, the variable values will likewise change in the SNL program. For recording motor positions, the level PV of a trigger signal for the detector is sensed. There are two states, 0 for non-collecting and 1 for collecting. When the trigger value is changed from 0 to 1, the motor current position is recorded. Conversely, when the trigger value is changed from 1 to 0, the motor current position is recorded again. The average value of the two motor positions is calculated in the SNL as the scan point position and is sent to top-layer SSCAN soft channels. Based on this method, the motor positions of each pixel are obtained. The data acquisition logic flow chart is shown in Fig. 3.

## 3 Results and discussion

At BL15U1 of the SSRF, elemental imaging of a standard gold mask was carried out using the new XRF scan system. The incident X-ray beam was monochromatized to 14 keV. The K-B mirror system was used to provide a focused beam with a spot size of 3.5 µm × 3.5 µm. Based on element contents of most samples for XRF experiment, 0.2 s scan time is enough to meet the actual requirements. The motor velocity was 7 µm/s. Scan range of the sample was arbitrarily selected using a microscope as shown in Fig. 4a. The motion path is shown in Fig. 4b. It can be seen that the entire trajectory is executed without stopping, saving the total experiment time dramatically relative to traditional 'step-by-step' mode. Elemental distribution images of the gold mask obtained are shown in Fig. 4c (the unit of color scale is intensity). Comparing Fig. 4a, c, the scanning area is the same. This shows that the method achieves irregular-shaped range mapping and confirms the presented method in this paper is valid.

Different scan modes of 'step by step,' 'table mode,' 'on-the-fly rectangle area' and 'arbitrary-shaped no-stopping' were used to measure this sample. The 'step-by-step' scan mode and 'table mode' cost 2621 and 2394 s, respectively, due to the motor start and stop at each scan position. On the contrary, the 'on-the-fly rectangle area' and 'arbitrary-shaped no-stopping' cost 857 and 684 s, respectively. The former took more time than the latter, because of the extra time to scan uninterested areas. The

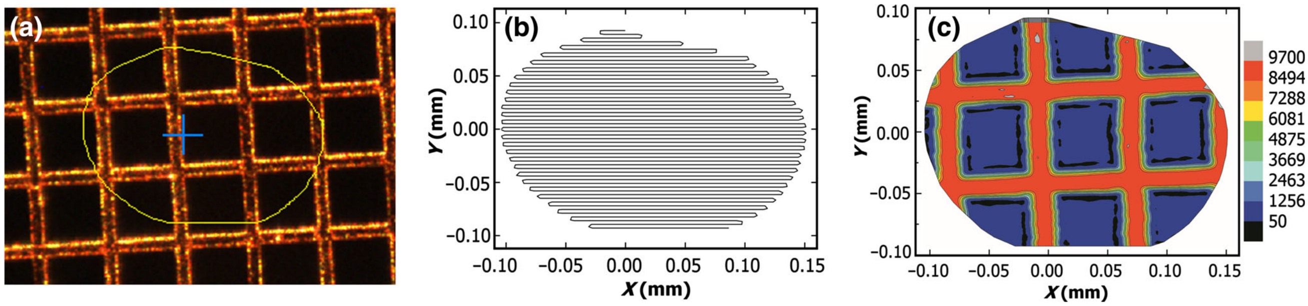


**Fig. 4** Selected area of a gold mask through microscope CCD (**a**), *X–Y* motion path of the motor (**b**), elemental mapping of the selected area (**c**)

'arbitrary-shaped no-stopping' scan mode is the most efficient scan method.

## 4 Conclusion

An effective SR-XRF scan method which maps irregular-shaped samples is provided in this paper. This scan mode gives a strategy to image elemental distributions of interested part of a sample. Based on this XRF scan, an elemental image of a standard gold mask was obtained with satisfactory results at BL15U1 of the SSRF. Compared to conventional scan methods, this scan pattern can not only achieve an arbitrary-shaped scanning based on a simply defined trajectory, but also allow the positioners to continuously move on the whole path without stopping. The experimental results show that the method is efficient to image elemental distributions and can save precious beam time for users. Additionally, the method also promotes the development of XRF methodology in the microfocusing beamline station.

## References


1. C.K. Bhat, D. Joseph, S. Pandita et al., Non-destructive analysis of didymium and praseodymium molybdate crystals using energy dispersive X-ray fluorescence technique. Radiat. Phys. Chem. **125**, 9–13 (2016). doi:10.1016/j.radphyschem.2016.02.028
2. M.L. Lord, F.E. McNeill, J.L. Grafe et al., A phantom-based feasibility study for detection of gadolinium in bone in vivo using X-ray fluorescence. Appl. Radiat. Isot. **112**, 103–109 (2016). doi:10.1016/j.apradiso.2016.03.021
3. I. Ramos, I.M. Pataco, M.P. Mourinho et al., Elemental mapping of biofortified wheat grains using micro X-ray fluorescence. Spectrochim. Acta Part B **120**, 30–36 (2016). doi:10.1016/j.sab.2016.03.014
4. J.H. Dycus, W. Xu, X. Sang et al., Influence of experimental conditions on atom column visibility in energy dispersive X-ray spectroscopy. Ultramicroscopy **171**, 1–7 (2016). doi:10.1016/j.ultramic.2016.08.013
5. M.A. Phedorin, V.A. Bobrov, K.V. Zolotarev, Peat archives from Siberia: synchrotron beam scanning with X-ray fluorescence measurements. Nucl. Instrum. Methods Phys. Res. Sect. A **575**, 199–201 (2007). doi:10.1016/j.nima.2007.01.067
6. K. Hayashi, N. Happo, S. Hosokawa, Applications of X-ray fluorescence holography to determine local lattice distortions. J. Electron Spectrosc. Relat. Phenom. **195**, 337–346 (2014). doi:10.1016/j.elspec.2014.07.008
7. L. Lu, J.W. Huang, D. Fan et al., Anisotropic deformation of extruded magnesium alloy AZ31 under uniaxial compression: a study with simultaneous in situ synchrotron X-ray imaging and diffraction. Acta Mater. **120**, 86–94 (2016). doi:10.1016/j.actamat.2016.08.029
8. F. Yan, *EPICS-Based Motion Control and Data Acquisition System on Synchrotron Radiation Microfocus Station*. Ph.D. Thesis (Shanghai Institute of Applied Physics, Chinese Academy of Sciences, Shanghai, 2011)
9. P. Wrobel, M. Czyzycki, L. Furman et al., Labview control software for scanning micro-beam X-ray fluorescence spectrometer. Talanta **93**, 186–192 (2012). doi:10.1016/j.talanta.2012.02.010
10. F. Yan, J.C. Zhang, A.G. Li et al., Fast scanning X-ray microprobe fluorescence imaging based on synchrotron radiation. Acta Phys. Sin. **60**(9), 1–7 (2011). doi:10.7498/aps.60.090702
11. S. Stepanov, H. Mark, W.Y. Derek et al., Fast fluorescence techniques for crystallography beamlines. J. Appl. Crystallogr. **44**, 772–778 (2011). doi:10.1107/S0021889811016748
12. Fast X-ray fluorescence imaging in continuous scanning mode at beamline L. http://hasyweb.desy.de/science/annual_reports/2005_report/part1/contrib/25/15448.pdf
13. P.M. Pelz, G. Sicairos, On-the-fly scans for X-ray ptychography. Appl. Phys. Lett. **105**, 251101 (2014). doi:10.1063/1.4904943
14. F.X. Kartner, F. Ahr, A.L. Calendron et al., AXSIS: exploring the frontiers in attosecond X-ray science, imaging and spectroscopy. Nucl. Instrum. Methods Phys. Res. Sect. A **829**, 24–29 (2016). doi:10.1016/j.nima.2016.02.080
15. J.M. Sampaio, T.I. Madeira, M. Guerra et al., Relativistic calculations of K-, L- and M-shell X-ray production cross-sections by electron impact for Ne, Ar, Kr, Xe, Rn and Uuo. J. Quant. Spectrosc. Radiat. Transf. **182**, 87–93 (2016). doi:10.1016/j.jqsrt.2016.05.012
16. XPS Series Universal High-Performance Motion Controller/Driver. http://www.newport.com/XPS-Series-Motion-Controllers-Universal-High-Perf/300904/1033/info.aspx
17. F. Yan, A.G. Li, K. Yang, EPICS-based data acquisition system of hard X-ray microfocus station. Nucl. Tech. **32**(11), 801–805 (2009). doi:10.7498/aps.60.090702
18. L.L. Zhang, S. Yan, S. Jiang et al., Hard X-ray micro-focusing beamline at SSRF. Nucl. Sci. Tech. **26**, 060101 (2015). doi:10.13538/j.1001-8042/nst.26.060101
19. T. Mooney, synApps:sscan. http://www.aps.anl.gov/bcda/synApps/sscan/sscan.html
20. B. Franksen, *State Notation Language and Sequencer*. http://www-csr.bessy.de/control/SoftDist/sequencer/